

Beam Optics Optimization in the KEK Digital Accelerator LEBT Considering the Effect of Remnant Magnetic Fields

Liu Xingguang^{#,A,B)}, Naoya Munemoto^{A,B)}, Ken Takayama^{A,B,C)}

^{A)} Tokyo Institute of Technology, 4259 Nagatsuta-cho, Midori-ku, Yokohama, Kanagawa 226-8503

^{B)} High Energy Accelerator Research Organization(KEK), 1-1 Oho, Tsukuba, Ibaraki 305-0801

^{C)} The Graduate University for Advanced Studies, Shonan Village, Hayama, Kanagawa 240-0193

Abstract

KEK Digital Accelerator is a compact induction synchrotron [1] which sets little limitation on the charged ion beam's species and injection velocities. Extracted from an Electron Cyclotron Resonance Ion Source (ECRIS), the ion beam ($A/Q=2, 4$) is transported through Low Energy Beam Transport (LEBT) line before injected into the ring for acceleration. As the velocity is relatively small ($\beta \sim 10^{-2}$), effects originating from remnant fields in different magnets along the LEBT line should be taken into account for orbit correction and optics optimization. With the help of online wire monitors, the following goals have been realized: (1) Beam orbit correction; (2) Twiss parameters and emittance at a chosen position are estimated; (3) beta function and injection focusing mismatch are studied with fitted results. These processes and results are presented and discussed in this paper.

INTRODUCTION

The layout of KEK Digital Accelerator (KEK DA) is shown in Fig. 1. The ECRIS is embedded in a 200kV high voltage platform to generate the ion beam. After transported through the LEBT Line, the extracted beam is kicked onto the orbit of the KEK DA Ring by an Electrostatic Kicker (ES Kicker) [2]. Eight combined-function type bending magnets are aligned for bending and transverse confinement of the beam while induction cells are installed for acceleration and confinement in the longitudinal direction. After acceleration, the ion beam is kicked out by the Extraction kicker and guided through Extraction Septum to the High Energy Beam Transport (HEBT) Line for beam related experiment. A detailed description of KEK DA can be found in [3].

Fig. 2 shows an example of the beam commissioning' survive rate plot for an $A/Q=4$ ion beam without acceleration, namely just free running of the beam after injection. While the overall beam loss could be attributed to the interaction between the beam and residual gas in the vacuum, the quick loss at the beginning is obvious. The most possible candidate responsible for this is optics mismatch happened at injection.

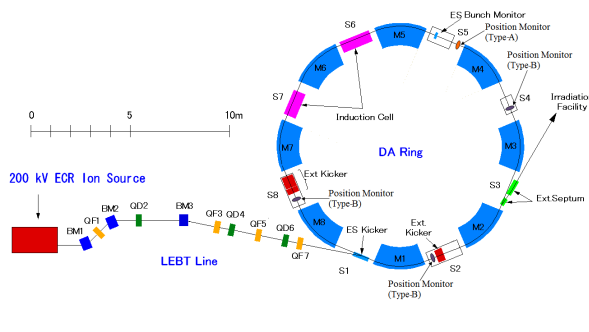


Figure 1: KEK DA layout

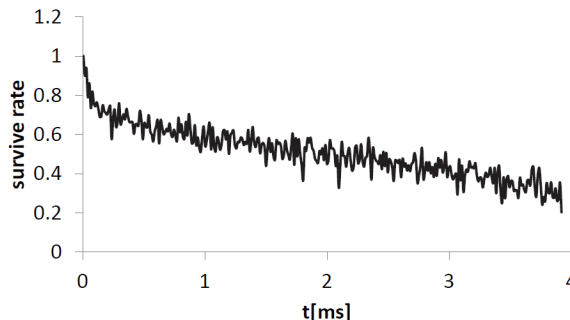


Figure 2: Survive rate in beam commissioning

Mismatch at injection is classified into two sorts of error. The first kind is steering error, where the injected beam is off-centred or tilted (or both), failing to sit on the right orbit. The other is optics focusing mismatch, where the profile of the injected beam in the phase space deviates greatly from the ring's lattice requirement.

The mismatch must be corrected or it would induce beam dilution in the phase space, in other words, emittance blow-up. Thanks to BPMs (Beam Position Monitor) installed in the ring, the steering error at injection could be identified by watching the coherent betatron oscillation in the ring and mitigated with the help of steering magnets before injection [4]. In contrast, focusing error has to be identified and corrected at the LEBT Line region. In this paper, the procedure of experiment and analysis is described to evaluate the lattice related parameters in LEBT Line using wire monitors, which have been restored to work this spring. Some results and discussion are given in estimating the seriousness of the focusing error and searching for solutions.

[#] liuxg@post.kek.jp

THEORETICAL BACKGROUND

The method described here is usually used to estimate the beam emittance experimentally, for example, in text book [5]. Considering the transverse motion of particle along a designed orbit in the LEPT, which consists of 3 bending magnets and 7 quadrupoles magnets as shown in Fig.3, the excursion of the particle position from the designed orbit and its angle are represented by (x, x') . Evolution of vector (x, x') along the orbit coordinate is expressed by,

$$\begin{pmatrix} x_1 \\ x_1' \end{pmatrix} = \begin{pmatrix} a_{11} & a_{12} \\ a_{21} & a_{22} \end{pmatrix} \begin{pmatrix} x_0 \\ x_0' \end{pmatrix} \quad (1)$$

where (x_0, x_0') and (x_1, x_1') are vectors at two positions of s_0 and s_1 (s is the coordinate along the designed orbit).

$\begin{pmatrix} a_{11} & a_{12} \\ a_{21} & a_{22} \end{pmatrix}$ is the transfer matrix between them. The transfer matrix for Twiss parameters (α, β, γ) , are written in the format of Eq. 2,

$$\begin{pmatrix} \beta_1 \\ \alpha_1 \\ \gamma_1 \end{pmatrix} = \begin{pmatrix} m_{11} & m_{12} & m_{13} \\ m_{21} & m_{22} & m_{23} \\ m_{31} & m_{32} & m_{33} \end{pmatrix} \begin{pmatrix} \beta_0 \\ \alpha_0 \\ \gamma_0 \end{pmatrix} \quad (2)$$

The relationship between Eq. 1 and Eq. 2 is,

$$\begin{pmatrix} m_{11} & m_{12} & m_{13} \\ m_{21} & m_{22} & m_{23} \\ m_{31} & m_{32} & m_{33} \end{pmatrix} = \begin{pmatrix} a_{11}^2 & -2a_{11}a_{12} & a_{12}^2 \\ -a_{11}a_{21} & a_{11}a_{22} + a_{21}a_{12} & -a_{12}a_{22} \\ a_{21}^2 & -2a_{21}a_{22} & a_{22}^2 \end{pmatrix} \quad (3)$$

In addition, the relationship between the beam size (denoted as 2σ) and the beta function is,

$$2\sigma = \sqrt{\varepsilon\beta} \quad (4)$$

where ε is the beam emittance. As a result, if we multiply both sides of Eq. 2 by ε (assuming emittance conservation along the beam line),

$$\begin{pmatrix} \varepsilon\beta_1 \\ \varepsilon\alpha_1 \\ \varepsilon\gamma_1 \end{pmatrix} = \begin{pmatrix} m_{11} & m_{12} & m_{13} \\ m_{21} & m_{22} & m_{23} \\ m_{31} & m_{32} & m_{33} \end{pmatrix} \begin{pmatrix} \varepsilon\beta_0 \\ \varepsilon\alpha_0 \\ \varepsilon\gamma_0 \end{pmatrix} \quad (5)$$

where $\varepsilon\beta_0$ and $\varepsilon\beta_1$ are the square root value of beam size at each position. The information of beam size is obtained from wire monitors located at different places.

The first one of the three independent equations in Eq. 5 is,

$$\varepsilon\beta_1 = m_{11}\varepsilon\beta_0 + m_{12}\varepsilon\alpha_0 + m_{13}\varepsilon\gamma_0 \quad (6)$$

By varying the focusing strength between two positions, (m_{11}, m_{12}, m_{13}) would change, while $(\varepsilon\beta_0, \varepsilon\alpha_0, \varepsilon\gamma_0)$ at starting point are constants. $\varepsilon\beta_1$ depends on the actual settings for magnets. Eq. 6 suggests that in order to solve three unknown parameters, three independent equations is sufficient enough. However, to reduce the error happened in this kind of estimation, it's usually better to take a series of data points then use fitting method to find these parameters. Choosing n cases of possible settings for Q magnets,

$$\begin{aligned} [\varepsilon\beta_1]^i &= m_{11}^i\varepsilon\beta_0 + m_{12}^i\varepsilon\alpha_0 + m_{13}^i\varepsilon\gamma_0 \\ i &= 1, 2, 3, 4, 5, \dots, n \end{aligned} \quad (7)$$

where $(m_{11}^i, m_{12}^i, m_{13}^i)$ and $[\varepsilon\beta_1]^i$ are the elements from the matrix in Eq. 5 for each setting of magnets.

$(\varepsilon\beta_0, \varepsilon\alpha_0, \varepsilon\gamma_0)$ could be obtained through fitting all the data. In addition, from the relationship among Twiss parameters, the emittance is written by,

$$\varepsilon = \sqrt{\varepsilon\beta_0\varepsilon\gamma_0 - \varepsilon\alpha_0^2} \quad (8)$$

EXPERIMENTAL SET-UP AND OBSERVATION

Set-up and wire monitors

Fig. 3 depicts the LEPT region, with positions of four wire monitors indicated (PR1 to PR4). Odd numberings of Q-magnet are focusing ones and even numberings defocusing for the horizontal direction. At present, Q3 and Q7 are excited in series with the same current. The Q4 and Q6 are excited in series with the same current as well.

The structure of the wire monitor is schematically shown in Fig. 4. It can measure the beam profile in the horizontal/vertical direction. Each of these wire monitors consists of a 32×32 wire grid as in the figure. These wires are so thin (diameters $\sim 30\mu\text{m}$) that they have little

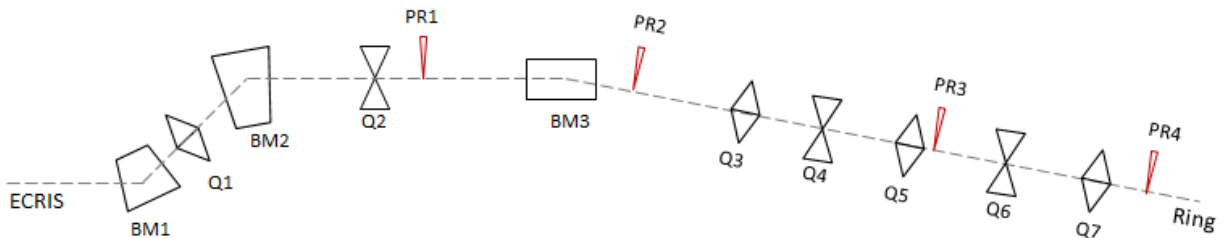


Figure 3: LEPT Line components and position of wire monitors

impact on the beam as the beam passes through. The distance between adjacent wires is 2.5mm, which also signifies the precision of the wire monitor. There are 32 channels for each direction and these channels are controlled with a series of gate signals.

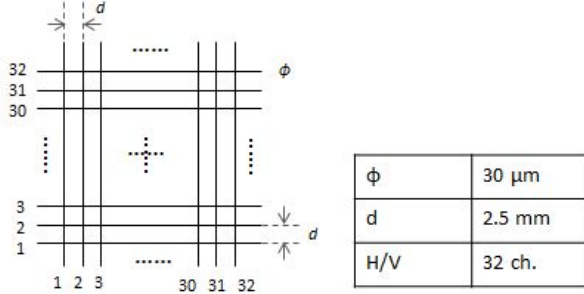


Figure 4: Structure of wire monitor

As an example, Fig. 5 shows screenshot of the beam signal taken by the wire monitor, in which ch1 is the gate signal and ch2 is the beam signal.

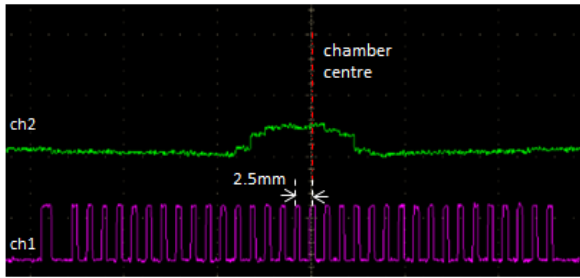


Figure 5: Gate signal (ch1) and beam profile (ch2)

At least two useful findings can be extracted from the wire monitor's measurement. The first one is whether the beam is located on the orbit centre, and if not, how much does the beam centre deviates from the designed orbit. The other one is that how the beam profile looks like. Assume that the beam profile is Gaussian like, Eq. 9 could be used to fit the profile, in which μ indicates the deviation of the fitted centre and σ reflects the beam size. For Gaussian distribution, the area between $\mu - 2\sigma$ to $\mu + 2\sigma$ is about 95% of the whole area, so in this paper, 2σ is used to stand for beam size (in fact, 2σ is only half width of the total beam size).

$$Ae^{-\frac{(x-\mu)^2}{2\sigma^2}} + C \quad (9)$$

Fig. 6 is a fitting result for Fig. 5, which shows that the deviation from the orbit centre is very small, less than 1mm, and the beam size in 2σ is about 0.6cm.

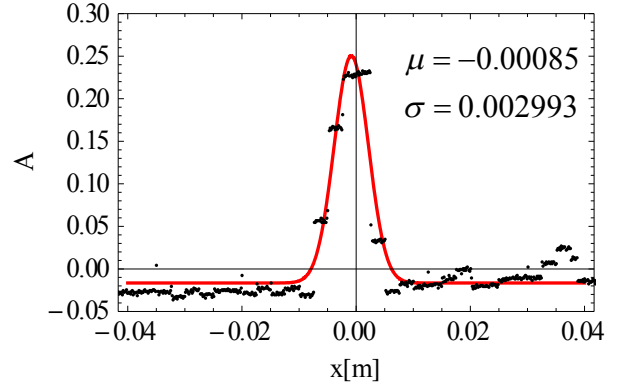


Figure 6: Gaussian fitting for Fig.5

Experimental observation

In our experiment, we use PR2 and PR4 (Fig.3) as the starting point (s_0) and observation point (s_1) to take the experimental data while changing the excitation currents for Q3~Q7. Different combinations used in the experiment are listed in Tab. 1.

Table 1: Excitation current for Q3~Q5

	Excitation Current(A)
$I_{Q3/Q7}^*$	7.8, 8.2, 8.7, 9.2
$I_{Q4/Q6}^*$	5.8, 6.4, 7.0, 7.6, 8.2
I_{Q5}	1.44, 1.96, 2.43

*Excited by the same power supply, so the excitation current are the same for Q3 and Q7, or Q4 and Q6

From Tab. 1 one sees that there are four values of Q3/Q7, five values of Q4/Q6, and three values of Q5. This yields a total possibility of 60 variations of the focusing strength between PR2 and PR4. All the beam profiles measured at PR4 under different settings of Q3~Q7 are laid out in Fig. 7 and Fig. 8, corresponding to the horizontal and vertical direction, respectively.

$(\epsilon\beta_0, \epsilon\alpha_0, \epsilon\gamma_0)$ in Eq. 7 are constants because the settings for upstream magnets were never changed through the experiment. The observation from PR4 (beam size in 2σ) corresponds to $[\epsilon\beta_1]^i$, where the case ID "i", starts from one to 60. The transfer matrix for Twiss parameters from PR2 to PR4, $(m_{11}^i, m_{12}^i, m_{13}^i)$, is evaluated by using the excitation currents $(I_{Q3/Q7}, I_{Q4/Q6}, I_{Q5})$. All quadrupole magnets are assumed the same type here. Field measurement result for one of the quadrupole magnets is available for the present purpose [6] and it is used for all the quadrupoles here. The k -value is related to the excitation current by,

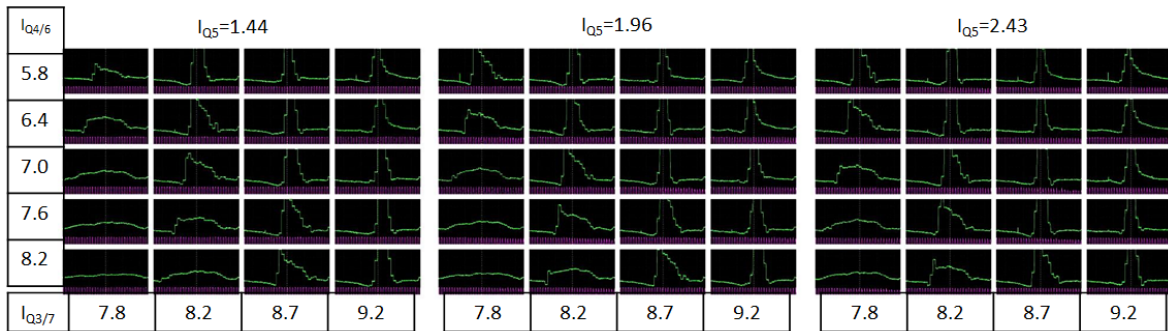


Figure 7: Experimental observation at PR4 in respect of excitation current (A), horizontal

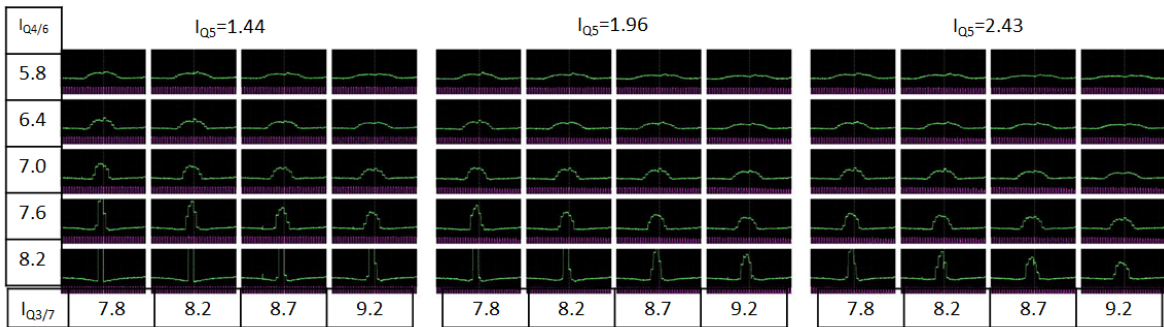


Figure 8: Experimental observation at PR4 in respect of excitation current (A), vertical

$$k = \frac{B'}{B\rho} \quad (10)$$

$$B' = g \times I[A] + b \quad (11)$$

where $g=0.0408$ and $b=0.0207$ according to the field measurement. Strictly speaking, different quadruple should have different excitation characteristics. All the quadruples on the present LEBT line had been used as magnets of the original KEK PS 40 MeV beam transport line and excited with higher currents. The gradient part, g , could be reasonably applied to all the quadruples while the remnant part, b , might vary somewhat due to their long time operation at different excitation current.

In this experiment, the beam has to be placed along the orbit centre so that the variation of focusing strength changes only the beam profile, but not the beam's position. Thus we have done the orbit centring by optimizing the settings for upstream magnets (before PR2).

DATA ANALYSIS

Fitting procedure

Though in total, there are 60 data sets, ($I_{Q3/Q7}, I_{Q4/Q6}, I_{Q5}, \epsilon\beta_1$ [or 2σ]) for each direction could be used for fitting for $(\epsilon\beta_0, \epsilon\alpha_0, \epsilon\gamma_0)$, considering that the precision of the wire monitors, to reduce the ambiguity, those data points with small beam size should be used with cautions. Thus, in the fitting process, only part of the data points is used. Especially for the horizontal direction

data, those data with too small beam size have been excluded in fitting.

With $g=0.0408$ and $b=0.0207$ and proper initial constraints, $(\beta_0, \alpha_0, \gamma_0)$ and ϵ in each direction are fitted as shown in Tab. 2.

Table 2: Fitted results at PR2

$\beta_x[m]$	α_x	γ_x	$\epsilon_x[\mu m.rad]$	$2\sigma_x[cm]$
3.32	-3.51	4.02	44.98	1.22
$\beta_y[m]$	α_y	γ_y	$\epsilon_y[\mu m.rad]$	$2\sigma_y[cm]$
2.48	1.44	1.24	24.78	0.78

The horizontal direction's fitted beam size at PR2 is almost the same as observed value (1.2cm). The vertical direction's fitted beam size at PR2 is slightly larger than the observed one (0.6cm). Another point worth mentioning here is that the horizontal emittance is larger than the vertical one, which is in accordance with our operation experience on LEBT line.

Fitting goodness

The goodness of fitting could be shown with plots of the beam size at PR4 calculated with fitted parameters and the real beam size observed in the experiment under the same fitting, as in Fig. 9 and Fig. 10. These comparisons suggest that though some errors unavoidably exist, overall speaking, the fitting is good.

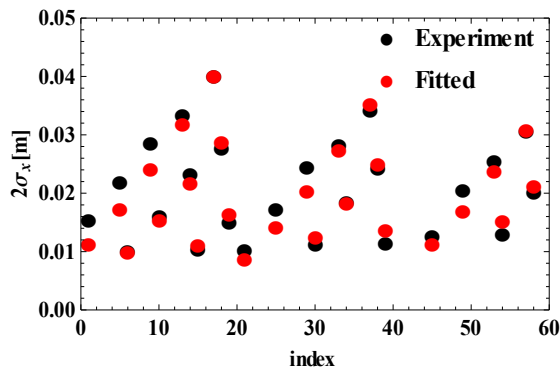


Figure 9: Comparison between fitted beam size and experimental results, horizontal

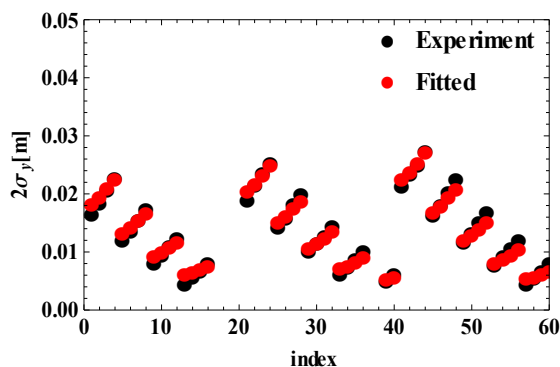


Figure 10: Comparison between fitted beam size and experimental results, vertical

The fitting residuals ($\Delta 2\sigma = 2\sigma_{\text{exp}} - 2\sigma_{\text{fitted}}$) are plotted in Fig. 11 for both directions. It's obvious that in Fig. 11 the residual points have almost the same trend with the original data, which might come from the fact that we simply used one equation for all the quadrupoles.

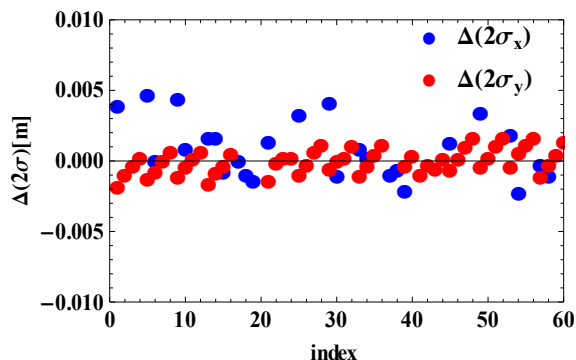


Figure 11: Residuals of fitting

However, at this moment, there's no enough information for each quadrupoles' excitation characteristics. Several cases have been tried by changing the remnant part, namely, b in Eq. 11 from 0.00 to 0.05 with stepwise of 0.01. Instead of plotting out all the residuals for different cases as in Fig. 11, the RMS of each case's residuals is shown in Fig. 12. This figure suggest that with all the remnant part assumed the same value, the present chosen one, 0.0207, is the best choice.

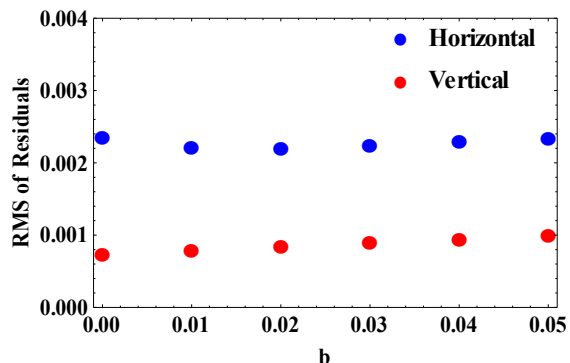


Figure 12: RMS residuals for various cases of b

DISCUSSION

Beta function in LEBT downstream and injection mismatch

With the fitted results from Tab. 2, under the settings for a typical case ($I_{Q3/7}=7.6A$, $i_{Q4/6}=7.0A$ and $I_{Q5}=2.3A$) that we used often for beam commissioning [7], the beta function from PR2 to the injection point of the Ring is calculated as shown in Fig. 13.

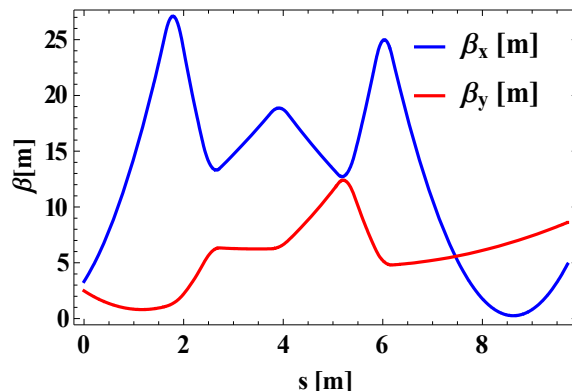


Figure 13: Beta function (LEBT region from PR2)

This figure suggests that the maximum beam size 2σ for x and y direction is $3.5cm$ and $2cm$, respectively, which are safely within the acceptance of LEBT vacuum chambers. At the place where the beam size is smallest, it is $0.7cm$ for horizontal and $0.5cm$ for vertical direction.

Table 3: Ring lattice at injection point

$\beta_x [m]$	α_x	γ_x
3.60	-0.22	0.29
$\beta_y [m]$	α_y	γ_y
1.90	-0.48	0.65

With calculated Twiss parameters at injection point, the seriousness of mismatch between LEBT lattice and Ring lattice is estimated. At the injection point, the Twiss parameters for both directions are given in Tab. 3 [3].

It is well known that if the injected beam has a different shape in the phase space as the ring lattice, the beam would diffuse in the phase space, resulting in a large emittance. Fig. 14 shows the mismatch between the LEBT lattice and Ring lattice under the present example settings for Q3~Q7. The blue-colour ellipse is the phase space for the ring lattice at the injection point, while the red-colour ellipse is the LEBT's. Under this mismatch and many perturbations such as nonlinear fields in the guiding magnet and space-charge forces, and ripples in the magnet power supply, eventually the beam would occupy the gray dotted ellipse indicated in the figure. After dilution process, the beam emittance has increased 13 times and 4 times for horizontal and vertical direction respectively. This mismatch may be able to explain the fast beam loss at the beginning as shown in Fig. 2.

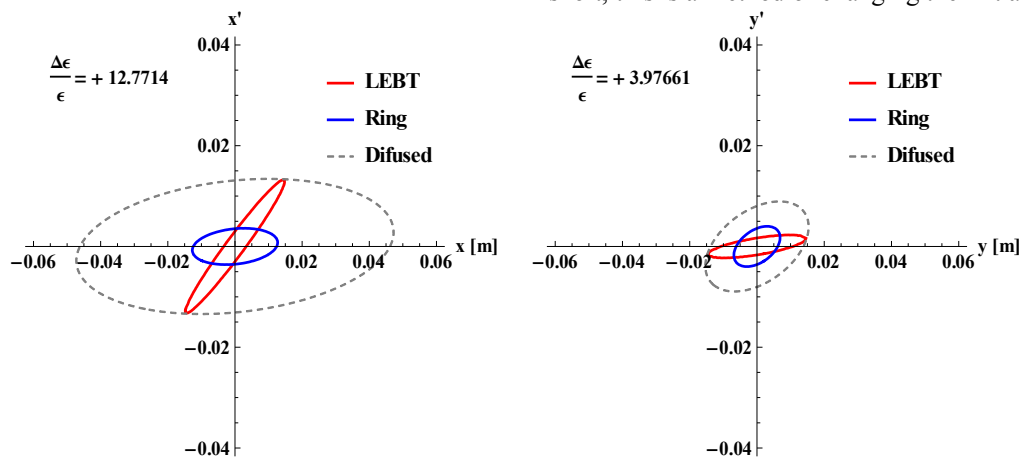


Figure 14: Mismatch between LEBT lattice and Ring lattice

SUMMARY AND FUTURE WORK

A complete process of estimating Twiss parameters and emittance with fitting method, including experimental set-up and data analysis was described in this paper. The fitted results could be used to study the beam Lattice in the LEBT region and more importantly to check the matching between LEBT lattice and Ring lattice. At present settings, the mismatch has a large possibility as the source for the fast beam loss at the injection in beam commissioning. This can be verified at next beam commissioning by observing the beam loss with different combinations of excitation currents for quadrupoles.

More experiments aiming at inspecting the applicability of the two possible solutions mentioned in last section are planned. It is expected that the fast beam loss at the beginning of beam commissioning could be mitigated after these work.

Possible solutions

Various combinations of ($I_{Q3/7}$, $I_{Q4/6}$, I_{Q5}) have been tried but failed to obtain the LEBT lattice optics to meet matching condition for both directions.

One solution is to increase degree of freedom of the magnet settings. As mentioned, Q3 and Q7 (also notice that they are located at both ends between PR2 and PR4) are excited with the same power supply, which means that for x direction, if a strong focusing force is applied to the Q3, the same focusing force emerges at Q7 location. The same thing happens for Q4 and Q6. Thus, if all quadrupoles are excited with independent power supplies, theoretically, matching for both directions could be realized.

Another solution comes by observing that the horizontal direction having a drastically changing of beta function magnitude is mainly due to the large angle (α_{x0}) at PR2. If this could be minimized by optimizing the upstream magnets, a better matching case could be found. In short, this is a method of changing the initial condition.

ACKNOWLEDGEMENT

This work is supported by a Grant-In-Aid for Scientific Research (A) (KAKENHI NO.23240082).

REFERENCE

- [1] K.Takayama, and J.Kishiro, *Nucl. Inst. Meth. Phys. Res. A* 451, 304 (2000).
- [2] T. Adachi and T. Kawakubo, *Phys. Rev. ST-AB* **16**, 053501 (2013).
- [3] T. Iwashita et al., *Phys. Rev. ST-AB* **14**, 071301 (2011).
- [4] T. Yoshimoto et al., in *Proc. of HIF2013* in Berkeley, August 12-17 (2012).
- [5] H. Wiedemann, *Particle Accelerator Physics (3rd Ed.)*, Sec. 5.1.
- [6] KEK DA Note 08-92 (*internal report*).
- [7] T. Yoshimoto et al., in this conference.